



ISSN: 0067-2904

Electron Collisions with Carbon Monoxide and Carbon Dioxide Molecules at a Wide Range of Energies.

Ahlam K. Yassir, Alaa A. Khalaf

Department of Physics, College of Science, University of Basrah, Basrah, Iraq

Received: 7/12/2022

Accepted: 27/6/2024

Published: 30/5/2025

Abstract

The present work displays a theoretical calculation of the differential, integral cross-sections, and momentum transfer of electrons scattering from carbon monoxide (CO) and carbon dioxide molecules (CO₂). The collision energy used ranged from 20 to 1100 eV for the CO molecule and from 10 to 700 eV for the CO₂ molecule. The partial wave analyses with complex optical model potential were used for solving the Dirac relativistic equation in the high and low energy regions. The results show decent agreement with current experimental studies and other theoretical predictions.

Keywords: electron scattering; carbon monoxide, carbon dioxide molecule; optical model potential; elastic Scattering

تصادم الإلكترونات بجزيئات أول أكسيد الكربون وثاني أكسيد الكربون على نطاق واسع من الطاقات.

احلام ياسر ، علاء خلف

قسم الفيزياء، كلية العلوم، جامعة البصرة، البصرة، العراق

الخلاصة

يبين العمل الحالي حساباً نظرياً للمقاطع العرضية التفاضلية والتكاملية ونقل زخم الإلكترونات المستطارة من جزيئة أول أكسيد الكربون (CO). وكذلك جزيئة ثاني أكسيد الكربون (CO₂). تراوحت طاقة التصادم المستخدمة من 20 إلى 1100 إلكترون فولت لجزيء أول أكسيد الكربون وأكسيد الكربون ومن 10 إلى 700 إلكترون فولت لجزيء ثاني أكسيد الكربون. تم استخدام التحليلات الموجية الجزيئية ذات الإمكانيات النموذجية البصرية المعقدة لحل معادلة ديرك النسبية. في مناطق الطاقة العالية والمنخفضة، تظهر النتائج اتقافاً جيداً مع الدراسات التجريبية الحالية والتنبؤات النظرية الأخرى. الكلمات المفتاحية: استطارة الإلكترون. جزيء أول أكسيد الكربون، جزيء ثاني أكسيد الكربون؛ موديل النموذج البصري؛ الاستطارة المرنة.

Introduction

Projectile and atom/molecule scattering is of great importance in many natural and man-made systems such as gaseous plasmas.[1]. Dispersion of ejected atoms or molecules is

*Email addressahlam.ashour.sci@uobasrah.edu.iq

highly common. Understanding scattering phenomena are critical for improving our knowledge of planetary sciences, stars, and interstellar space and developing technologies[2, 3]. However, it is important to study electron impact scattering from atmospheric molecules using models of both chemistry and physics, like gas transport electrons, atmospheric auroral, photochemistry of the atmosphere, emissions, biomaterial treatment, and plasma discharges[4]. Compounds that contain carbon, such as carbon monoxide and carbon dioxide, are the most essential material in the atmosphere and are the main factor of the chemistry that occurs in the atmosphere[5].

Carbon monoxide (CO) is a major component of the atmosphere molecules of Venus and Mars[6]. It is a known component of comets in interstellar space. Furthermore, CO is used for gaseous discharges in the laboratory for different purposes[7]. On the other hand, electron-carbon monoxide collisions play an important role in research on these topics, and now a large number of new cross-section data are available[8, 9].

Carbon dioxide (CO₂) is a linear triatomic, nonpolar, and heterogeneous molecule. It is the most available component of Venus and Mars atmospheres and on earth [10]. However, to understand the aurora borealis and daylight, the excitation cross-sections, ionization, and dissociation of atmospheric types by electrons should be understood [7]. Therefore, reliable statistics of the electron-CO₂ (e-CO₂) collisions are important for controlling the atmosphere. Moreover, CO₂ is often used in gaseous vacuums and low-temperature plasma devices. Thus, many experimental and theoretical articles regarding e-CO₂ dispersal were collected and published until 2022 by a review article [8, 10-13]. Billah et al. [14] studied e-CO₂ dispersal at a threshold energy of 10,000 eV, while Vinodkumar et al.[15] calculated e-CO₂ dispersal at 5000 eV. Recently, Hudson et al.[16] studied the e-CO₂ dispersal at a threshold energy of 250 eV and estimated the total inelastic cross-section depending on the famous Spherical Complex Optical Potential (SCOP) formula.

The study of differential cross sections of CO and CO₂ obtained a new set of recommended cross-sections. The independent atom model and screening correction using a complicated optical potential were used for solving Dirac relativistic equation in partial-wave[17]. The model successfully calculated various observables of electrons and positrons scattering from CO molecule targets.

In the present work, Differential Cross Sections (DCS), Total Cross Sections (TCS) and Momentum Transfers Cross Sections (MTCS) of the electron scattering from CO and CO₂ molecules at energy ranging from 20eV to 1100eV were calculated. Furthermore, the spin polarization of these scattering systems was determined for the first time. Dirac theory and the partial wave analysis with a complicated optical potential model were used in our calculations to adapt the fractional wave approach to the projectile-molecule interaction [18].

2. Theory

Partial wave action cannot be used to determine the scattering of electrons by a molecule because of the non-spherical shape of the shell molecule connection. The dispersion of the cross-sections because of the molecule (differential or integral) is created by simply adding the special contribution made by the individual free atoms that comprise the molecule according to the Additive Rule (AR)[14], which represents a basic approximation involving chemical bonding and aggregation effects. However, when an identical atom is present in a molecule, its intensity distribution differs from its density distribution when the atom is alone, where the grouping in the molecular composition leads to a distortion in the density distribution, which has an impact on dispersion as well as on the projectile and molecule

interaction of the atom-shell. The interaction of atoms in a molecule results in the formation of a free atom in the independent atom approximation and a reduction of single center dispersion of a molecule to a polycentric dispersion of a symmetric spherical potential owing to a free atom. The approximation allows the use of scattering partial wave analytics. This method can account for the molecular impact by defining the differential cross-section as a cohesive collection of waves transmitted from atoms at fixed points inside the molecule[17]. In addition, instead of the atom, the energy of the initial excitation and the dipole polarizability of the molecule are utilized to form the projectile atom. According to a theoretical framework, the contraction of the scattering potential is a critical problem that affects the calculated scattering parameters when a complex potential is present as an optical potential. Therefore, scattering potential contraction was investigated and identified[14].

The relativistic Dirac formula [19] of a projectile of m_0 rest mass moving in a central field of $V(r)$ with a velocity of v is given by:

$$[\alpha \mathbf{p} + \beta m_0 c^2 + V(r)] \psi(r) = \varepsilon \psi(r) \quad (1)$$

$$\varepsilon = \gamma m_0 c^2 = \varepsilon_i + m_0 c^2$$

the total energy is:

$$\gamma = (1 - v^2/c^2)^{-1/2}$$

Where: c is the speed of light in vacuum, ε_i is the kinetic energy of the incident particle and α and β are the usual 4×4 Dirac matrices.

Potential visual complexity

The package of radial subroutines [20] and the complicated optical potential [21] type were used for solving the Dirac equation numerically:

$$V(r) = V_{real}(r) - iW_{abs}(r)$$

$$= V_{st}(r) + V_{ex}(r) + V_{cp}(r) - iW_{abs}(r) \quad (2)$$

The exchange, static, and correlation polarization potentials are represented by the genuine elements $V_{ex}(r)$, $V_{st}(r)$ and $V_{cp}(r)$, respectively, while the amplitude of the absorption potential is represented by the imaginary component $W_{abs}(r)$. An electron's overall interaction with a target atom is described by the effective potential $V(r)$ selected to be the three potentials added together; static $V_{st}(r)$, exchange $V_{ex}(r)$, and the correlation-polarization $V_{cpol}(r)$ potentials. The terms are functions of the target's electronic density and approximate the collision dynamics given by:

$$V(r) = V_{st}(r) + V_{ex}(r) + V_{cor}(r) + V_{pol}(r) \quad (2)$$

The energy of the projectile's electrostatic interaction with the target atom can be obtained through [22]:

$$V_{st}(r) = Z_0 e \phi(r) = Z_0 e [\phi_n(r) + \phi_e(r)] \quad (3)$$

$$V_{st}(r) = Z_0 e \phi(r) = Z_0 e [\phi_n(r) + \phi_e(r)] \quad (4)$$

$$\phi(r) = \phi_e(r) + \phi_n(r) \quad (6)$$

$$\phi_e(r) = -e \left[\frac{1}{r} \int_0^r 4\pi r'^2 \rho_e(r') dr' + \int_r^\infty 4\pi r' \rho_e(r') dr' \right] \quad (5)$$

$$\phi_n(r) = e \left[\frac{1}{r} \int_0^r 4\pi r'^2 \rho_n(r') dr' + \int_r^\infty 4\pi r' \rho_n(r') dr' \right] \quad (6)$$

Where: $Z_0 e$ is the charge of the projectile electrons ($Z_0 = -1$), r is the distance from centre of the molecule, $\phi(r)$ is the electrostatic potential function of the target atom represented as the

sum of the nucleus' and electron's contributions which is the total contribution from the nucleus and electron cloud, and $\Phi_n(r)$ and $\Phi_e(r)$ are formed by the distribution of electric and nuclear charge, respectively [20] produced as a result of the electronic and nuclear charge distributions, respectively. The Fermi nuclear charge distribution $\rho_n(r)$, provided by Hahn et al. [23]. Was used to create $\Phi_n(r)$. Furthermore, $\rho_e(r)$ was generated using the most exact electron densities, while $\Phi_e(r)$ is available for free atoms, which are determined from self-consistent relativistic Dirac-Fock (DF) computations [18]. The electron exchange potential was calculated by the same density of $\Phi_e(r)$. The exchange potential model of Furness and McCarthy [24], that is a local approximation to the exchange interaction, was used to do the computations that is provided by:

$$V_{ex}(r) = \frac{1}{2}(E_i - V_{st}(r)) - \frac{1}{2}[(E_i - V_{st}(r))^2 + 4\pi a_0 e^4 \rho_e(r)]^{1/2} \quad (7)$$

Where: E_i , is the projectile's kinetic energy and a_0 is the first Bohr radius. The parameter of free polarization potential for the binding and polarization potential $V_{cpol}(r)$ can be determined by the binding energy of the target molecule as provided by Salvat et al. [20] where it has two components: short-running $V_{cor}(r)$ and long-running $V_{pol}(r)$ parts.

$$V_{cpol}(r) = \begin{cases} V_{cor} & \text{if } r < r_c \\ V_{pol} & \text{if } r \geq r_c \end{cases} \quad (8)$$

The present work has adopted the parameters of the correlation potential given by O'Connell and Lane [25]

$$2v_c[\rho] \equiv \begin{cases} 0.0622 \ln r_s - 0.096 + 0.018 r_s \ln r_s - 0.02 r_s & r_s \leq 0.7 \\ -0.1231 + 0.03796 \ln r_s, & 0.7 < r_s \leq 10 \\ -0.876 r_s^{-1} + 2.65 r_s^{-3/2} - 2.8 r_s^{-2} - 0.8 r_s^{-5/2}, & 10 \leq r_s \end{cases} \quad (9)$$

Where:

$$r_s = \left(\frac{3}{4\pi\rho} \right)^{1/3} \quad (10)$$

The projectile's electrostatic interaction with a static potential is caused by the atomic charge distribution that can produce electron density calculated using Dirac-Focus [26] and the nuclear charge distribution of Fermi [23]. The present work used Furness and McCarthy's [24] quasi-classical local exchange potential constructed from non-local exchange interactions utilizing WKB-like wave functions. The potential for polarization occurs as a consequence of the displacement of the atom's charges by the charged event and remains attractively ejected to both electrons. Gote and Ehrhardt [27] used the $V_{cp}(r)$ global correlation-polarization potential, which blends long-range Buckingham potentials with no parameters and short-range correlation potentials based on Local Density Approximation (LDA). For projectiles with kinetic energy above the first excitation threshold, there is a loss of particles from the elastic channel to inelastic channels. This effect can be modelled by including a negative imaginary term, $-iW_{abs}(r)$, in the optical-model potential. $-iW_{abs}(r)$.

The $V_{st}(r)$, $V_{ex}(r)$, $V_{cp}(r)$, and $W_{abs}(r)$ components were shown in detail by many published works [17, 28, 29]. In the Dirac partial wave analysis, elastic scattering amplitude completely describes electron scattering by the potential $V(r)$ [30]. Two contributions can be referred to: the spin-conserving contribution, $F(\theta)$, and the spin-flip contribution, $g(\theta)$. The elastic differential cross section of a non-polarized electron can be calculated using:

$$\frac{d\sigma}{d\Omega} = |\mathbf{f}(\boldsymbol{\theta})|^2 + |\mathbf{g}(\boldsymbol{\theta})|^2 \quad (11)$$

Because the projectile-molecule interaction is not spherically symmetric, the partial-wave method cannot be used to directly generate observable numbers for e-CO, CO₂ scattering. The amplitudes of direct and spin-flip scattering are calculated using[17]:

$$\mathbf{f}(\boldsymbol{\theta}) = \sum_i \exp(i\mathbf{q} \cdot \mathbf{r}_i) \mathbf{f}_i(\boldsymbol{\theta}) \quad (12)$$

And

$$\mathbf{g}(\boldsymbol{\theta}) = \sum_i \exp(i\mathbf{q} \cdot \mathbf{r}_i) \mathbf{g}_i(\boldsymbol{\theta}) \quad (15)$$

Where: $i\mathbf{q}$ represents the momentum transfer, \mathbf{r}_i is the position vector of an atom i 's nucleus with reference to an arbitrary origin, and $\mathbf{f}_i(\boldsymbol{\theta})$ and $\mathbf{g}_i(\boldsymbol{\theta})$ are the scattering amplitudes of the element's component-free atom. The appropriate DCS is calculated by the average of the orientations of all random oriented particles and are given by:

$$\frac{d\sigma}{d\Omega} = \langle |\mathbf{F}(\boldsymbol{\theta})|^2 + |\mathbf{G}(\boldsymbol{\theta})|^2 \rangle \quad (13)$$

$$= \sum_{i,j} \exp(i\mathbf{q} \cdot \mathbf{r}_{ij}) [\mathbf{f}_i(\boldsymbol{\theta}) \mathbf{f}_j^*(\boldsymbol{\theta}) + \mathbf{g}_i(\boldsymbol{\theta}) \mathbf{g}_j^*(\boldsymbol{\theta})] \quad (14)$$

$$= \sum_{i,j} \frac{\sin(qr_{ij})}{qr_{ij}} [\mathbf{f}_i(\boldsymbol{\theta}) \mathbf{f}_j^*(\boldsymbol{\theta}) + \mathbf{g}_i(\boldsymbol{\theta}) \mathbf{g}_j^*(\boldsymbol{\theta})] \quad (15)$$

$$= \sum_i [|\mathbf{f}_i(\boldsymbol{\theta})|^2 + |\mathbf{g}_i(\boldsymbol{\theta})|^2] + \sum_{i \neq j} \frac{\sin(qr_{ij})}{qr_{ij}} [\mathbf{f}_i(\boldsymbol{\theta}) \mathbf{f}_j^*(\boldsymbol{\theta}) + \mathbf{g}_i(\boldsymbol{\theta}) \mathbf{g}_j^*(\boldsymbol{\theta})] \quad (16)$$

In this equation, $q = 2k \sin \theta/2$, r_{ij} is the distance between the atoms located at the i -th and j -th positions. $\sin \frac{(qr_{ij})}{qr_{ij}} = 1$ when $qr_{ij} = 0$ and the expression $\sum_{i \neq j}$ reflects interference's contribution to molecular DCS. The integrated elastic (σ_{el}), momentum-transfer (σ_m), and viscosity (σ_v) cross-sections for e - CO, CO₂ scattering are expressed in terms of DCS as:

$$\sigma_{el} = \int \frac{d\sigma}{d\Omega} d\Omega = 2\pi \int_0^\pi \left(\frac{d\sigma}{d\Omega} \right) \sin(\theta) d\theta \quad (17)$$

$$\sigma_m = 2\pi \int_0^\pi (1 - \cos\theta) \left(\frac{d\sigma}{d\Omega} \right) \sin(\theta) d\theta \quad (18)$$

$$\sigma_v = 3\pi \int_0^\pi [1 - (\cos\theta)^2] \left(\frac{d\sigma}{d\Omega} \right) \sin(\theta) d\theta \quad (19)$$

The total cross-section for the projectiles can be calculated by:

$$\sigma_{tot} = \frac{4\pi}{k} \sum_i \text{Im} f_i(0) \quad (20)$$

Where: $\text{Im} f_i(0)$ refer to the imaginary component of the forward direct of scattering amplitude $\theta=0$ for i -th atom. The σ_{tot} includes both elastic and inelastic (absorption) portions due to the imaginary component. The inelastic cross-section in is given by:

$$\sigma_{inel} = \sigma_{tot} - \sigma_{el} \quad (21)$$

The Independent Atom Model (IAM) model has a flaw in that it does not account for multiple scattering of the shells from the molecule's constituent atoms, that limits its applicability to relatively high energies higher than 100eV [17, 31]. Another reason for this low-energy model's failure is its lack of knowledge of mutual interference between adjacent atomic cross-sections. To solve the problem, Blanco et al. [31]. presented s_i -correcting assay ($0 \leq s_i \leq 1$) for a molecule's i -th and j -th atoms, that is provided by:

$$s_i = 1 - \frac{\epsilon_i^{(2)}}{2_i} + \frac{\epsilon_i^3}{3_i} - \frac{\epsilon_i^4}{4_i} + \dots \mp \frac{\epsilon_i^N}{N_i} \tag{22}$$

Where (26)

$$E_i^{(m)} = \frac{N - m + 1}{N - 1} \sum_{i \neq j}^{\sigma} \frac{j \epsilon_j^{(m-1)}}{\alpha_{ij}} \quad (m = 2, \dots, N)$$

m represents the number of interfering atoms and N is the number of the atom in the target molecule, and $ij = \max(4\pi r_i r_j, \sigma_i \sigma_j)$ where i and j are atomic total cross sections of the molecule's i-th, j-th atoms. Equation (15) has the following form for a CO₂ molecule (N=3) and CO molecule (N=2):

$$s_i = 1 - \frac{\epsilon_i^{(2)}}{2!} + \frac{\epsilon_i^{(3)}}{3!} \tag{23}$$

However, These coefficients S_i reduce the contributions of constituent atoms to the molecular cross-section Blanco et al. [31] improved the formalism by adding another factor, V_{ij}, to the positive values of :

$$\sum_{i \neq j} v_{ij} s_i s_j \frac{\sin(qr_{ij})}{qr_{ij}} [f_i(\theta) f_j^*(\theta)],$$

which is defined by

$$v_{ij} = r_{ij}^2 / (r_{ij}^2 + \rho_{ij}^2),$$

with a length-dimensional parameter

$$\rho_{ij} = \max\left(\frac{\sqrt{\sigma_i}}{\pi}, \frac{\sqrt{a_j}}{\pi}, \frac{1}{k}\right). \text{ Here, } (\sqrt{\sigma/\pi}) \text{ depicts the radius of an area circle. As a result,}$$

Equation[32] was screening-corrected:

$$\left(\frac{d\sigma}{d\Omega}\right)^s = \sum_i s_i^2 [|f_i(\theta)|^2 + |g_i(\theta)|^2] + \sum_{i \neq j} v_{ij} s_i s_j \frac{\sin(qr_{ij})}{qr_{ij}} \left[\begin{matrix} f_i(\theta) f_j^*(\theta) + \\ g_i(\theta) g_j^*(\theta) \end{matrix} \right] \tag{24}$$

The screening-corrected integrated elastic σ_{el} , momentum-transfer σ_m , viscosity σ_v , and total σ_{tot} cross-sections are given by:

$$\sigma_{el}^s = 2\pi \int_0^\pi \left(\frac{d\sigma}{d}\right)^s \sin(\theta) d(\theta) \tag{25}$$

RESULTS

Relativistic calculation of the Total Cross Sections (TCSs), Differential Cross Sections (DCSs), and momentum transfer for electrons collisions with CO and CO₂ molecules in various energies of (20-1100) eV for CO and (10-700) eV for CO₂ employing optical model potential was done. The calculations were carried out using both real and absorption potentials. Tables 1&2 list the calculated scattering values of MTCS, TCS for the e-CO and e-CO₂, respectively

Figure 1 shows the obtained results of DCSs for e-CO collisions at 20 eV compared with the theoretical data of Billah et al. [17], Castro et al. [33], Lee et al. [34] and the experimental data of Middleton et al. [35], and Nickel et al. [36]. For the energy of 25eV, the obtained results were compared with the data of Billah et al. [17] and the measurements of Gote and Ehrhardt [27]. For the energy 30eV, the results were compared with the data of Billah et al. [17], Lee et al.[34], and the measurements of Gibson et al. [37], Middleton et al.[35], and Chutjian and Tanaka [38]. The results for the 40eV energy were compared with the data of Billah et al. [17] and the measurements of Middleton et al. [35], Nickel et al. [36] and Chutjian et al. [38].

Figure 2 shows the obtained DCS results at 50 eV energy, which were compared with the theoretical data of Billah et al. [17], Castro et al.[33] and Lee et al. [34], the results were also compared with the experimental data obtained from Middleton et al. [35], Nickel et al. [36] and Gote and Ehrhardt [27]. The results for the energies of 60eV and 70eV were compared with the data of Billah et al. [17] and the measurements obtained by Nickel et al. [36]. The 75 eV energy results were compared with the data of Billah et al. [17], Lee et al. [34] and with the experimental data of Gote and Ehrhardt [27].

Figure 3 compared the results of DCSs at 80eV and 90eV with the theoretical data of Billah et al. [17] and the experimental data of Nickel et al. [36], while the results of the 100eV energy were compared with the data of Billah et al. [17] and with the experimental data of Nickel et al.[36], Castro et al. [33], and Lee et al.[34]. Finally, for the energy of 125eV, the results were compared with the data of Billah et al. [17] and with the experimental data of Gote and Ehrhardt [27].

Figure 4 shows the results of DCSs at 150 eV and 200eV compared with the theoretical data of Billah et al. [17], and with the experimental data of Gote and Ehrhardt [27]. For the energy 175eV, the results were compared with the data of Billah et al. [17] and the experimental data of Gote and Ehrhardt [27]. For higher energy of 200eV, the results were compared with the data of Billah et al. [17], Lee et al. [34], and with the experimental data of Gote and Ehrhardt [27]. For the energy of 300eV, the results were compared with the data of Billah et al. [17] and Lee et al. [34] and with the experimental data of Maji et al. [39] and Bromberg [40].

Figure 5 shows the obtained results of DCs at 400 eV compared with the theoretical data of Billah et al. [17] and Jain [41] as well as with the experimental data of Bromberg et al. [40]. The 500 eV energy results were compared with the data of Billah et al. [17], Lee et al. [34] and with the empirical data of Maji et al.[39] and DuBois and Rudd [42]. Furthermore, the energy 700eV results were compared using the data of Billah et al. [17] and Maji et al. [39] and with the experimental data of Maji et al.[39]. Finally, the 800eV energy results were compared by the data of Billah et al. [17], Jain [41] and with the experimental data of DuBois and Rudd [42].

Figure 6 shows the results of DCSs at 900 and 1100eV compared with the theoretical data of Billah et al.[17], Maji et al. [39] and with the experimental data of Maji et al.[39].

The TCS and TMCS results are shown in Figure 7(a and b), respectively. The TCS results were compared with the theoretical data of Kanik et al.[43] and Jain and Baluja [44] and the results were compared with the experimental data of Gibson et al.[37]. Moreover, the results of TMCS were compared with the theoretical data obtained by Jain and Baluja [44] and Morgan and Tennyson [45] and with the experimental data of Gibson et al. [37] and Haddad and Milloy[46].

Figure 8 shows the DCSs results of e-CO₂ collision at 10 eV compared with the theoretical data of Lee et al. [47], Morrison et al. [48], and with experimental data of Tanaka et al. [49] and Srivastave et al.[50]. The obtained results at energy 20 eV were compared with the data of Lee et al.[47] and Gianturco and Paoletti [51], as well as with the experimental data of Tanaka et al. [49] and Gibson et al.[37]. The 30 eV energy results were compared with the data of Botelho et al. [4] and with the experimental data of Tanaka et al. [49] and Gibson et al. [37]. For the energy of 40 eV, the results were compared with the data of Billah et al.[14] and with experimental data of Tanaka et al. [49], Shyn et al.[52] and Gibson et al.[37].

The results of DCSs at 50 eV are shown in Figure 9 and are compared with the theoretical data of Billah et al. [14] and Botelho et al. [4] and with the experimental data of Register et al.[53], Shyn et al.[52] and Gibson et al. [37]. For the 60 eV energy, the obtained results were compared with the data of Billah et al.[14] and Iga et al.[54] and with the experimental data of Tanaka et al.[49]. The results obtained with 70eV energy were compared with the data of

Billah et al. [14] and with the experimental of Kanik et al. [55] and Shyn et al.[52]. For the energy of 80eV, the results were compared with those obtained by Billah et al.[14] and with the experimental data of Kanik et al. [55].

The results of DCSs obtained at 90 eV were compared with the theoretical data of Billah et al. [14] and Botelho et al.[4] and with the experimental results of Register et al.[53]. For the energy of 100eV, the results were compared with the data of Billah et al.[14] and Iga et al.[54] and with the experimental data of Iga et al.[54]. The results with energy 200eV were compared with Billah et al. data[14] and Iga et al.[54] and also with the experimental data of Iga et al.[54]. For the energy of 300eV, the obtained results were compared with the data of Billah et al. [14] and Botelho et al.[4] and with the experimental data of Iga et al.[54, 56]. Figure 11 shows the results of DCSs at 400eV, which were compared with the theoretical data of Billah et al. [14] and with the experimental data of Bromberg [57] and Iga et al. [54]. The 500eV energy results were compared with the data obtained by Billah et al.[14] and Botelho et al.[4] and with the experimental data of Bromberg [57] and Iga et al.[56]. The results of energy 600 eV were compared with data of Billah et al. [14]. The results of the energy 700 eV were compared with the Billah et al. results[14] and with the experimental results of Maji et al.[39].

The results of TCS are shown in Figure 12a and were compared with the theoretical data of Billah et al. [14], De-Heng et al. [58] and Jain and Baluja [44] as well as with the experimental data of Szmytkowski and Maciąg [59]. Figure 12b compares the TMCS obtained results with the theoretical data of Billah et al. [14] and Nakamura [60] and with the experimental data of Gibson et al.[37].

It is noteworthy that at $E_i < 10$ eV of the TCS no theoretical calculations can produce the resonance shape. However, Theoretical works, such as the R-matrix or multi-channel computations, can re-produce these special low-power features.

DISCUSSION:

Interference structures are caused by the way the DCS changes with angle (or energy), which appear only in low-energy fields. These structures are of great interest in collision dynamics where they appear because of the diffraction effects emerging from the quantum mechanics nature of matter. However, the interference structures are absent when a collision becomes very energetic, leading to the interactions of molecules and projectiles to occur inside the K shell. The DCs results calculated from Figures 8 to 11 were done at different energies at which the projectile's de Broglie - wavelengths are tiny enough in comparison to the target molecules' interatomic distances. Therefore, incident particles collide with all the atoms (within the target molecule) separately, with no geometrical overlap.

In general, the obtained results of DCSs for e-CO collision with different energies very well agreed with those obtained by others. For e-CO₂ collision at low energies, some differences were noted between our results and those of other researcher. However, at intermediate and high energies, the results were enhanced. Furthermore, according to total and momentum transfer cross results presented in Figures 7 &12, the TCs results appeared good except at high energies where some discrepancy for the MTCs was noticed.

Table 1 : momentum-transfer (MTCS) and total (TCS) cross-sections for e-CO scattering.

Energy (eV)	TCS (cm ²)	MTCS(cm ²)
1.00000E+01	2.22379E-15	1.58463E-15
2.00000E+01	1.64124E-15	1.12327E-15
3.00000E+01	1.25941E-15	7.70175E-16
4.00000E+01	1.04812E-15	5.89322E-16
5.00000E+01	9.07630E-16	4.72224E-16
6.00000E+01	8.04441E-16	3.88075E-16
7.00000E+01	7.23987E-16	3.25071E-16
7.50000E+01	6.89807E-16	2.99433E-16
8.00000E+01	6.59278E-16	2.76932E-16
9.00000E+01	6.07063E-16	2.39492E-16
1.00000E+02	5.64025E-16	2.09844E-16
1.25000E+02	4.82955E-16	1.57583E-16
1.50000E+02	4.25847E-16	1.24046E-16
1.75000E+02	3.83752E-16	1.01370E-16
2.00000E+02	3.50824E-16	8.49867E-17
3.00000E+02	2.65889E-16	4.90366E-17
4.00000E+02	2.16850E-16	3.29625E-17
5.00000E+02	1.83776E-16	2.40712E-17
7.00000E+02	1.42077E-16	1.47403E-17
8.00000E+02	1.27886E-16	1.20586E-17
9.00000E+02	1.16364E-16	1.00718E-17

Table 2: momentum-transfer (MTCS) and total (TCS) cross-sections for e-CO₂ scattering

Energy (eV)	TCS (cm ²)	MTCS (cm ²)
6.00000E+00	2.66383E-15	1.26419E-15
8.00000E+00	2.64889E-15	1.28111E-15
9.00000E+00	2.61737E-15	1.28347E-15
1.00000E+01	2.57729E-15	1.28190E-15
1.50000E+01	2.33059E-15	1.22339E-15
2.00000E+01	2.09317E-15	1.12577E-15
2.50000E+01	1.89375E-15	1.02416E-15
3.00000E+01	1.72891E-15	9.28943E-16
3.50000E+01	1.59149E-15	8.42616E-16
4.00000E+01	1.47578E-15	7.65780E-16
4.50000E+01	1.37720E-15	6.97804E-16
5.00000E+01	1.29237E-15	6.38019E-16
6.00000E+01	1.15407E-15	5.39276E-16
6.50000E+01	1.09694E-15	4.98405E-16
7.00000E+01	1.04489E-15	4.62179E-16
8.00000E+01	9.55841E-16	4.00963E-16
9.00000E+01	8.82832E-16	3.51568E-16
1.00000E+02	8.21912E-16	3.11315E-16
2.00000E+02	5.13350E-16	1.30991E-16
3.00000E+02	3.88976E-16	5.22475E-19
4.00000E+02	3.18054E-16	4.12856E-19
5.00000E+02	2.70540E-16	3.35197E-19
6.00000E+02	2.36446E-16	2.78059E-19
1.50000E+03	1.14085E-16	7.19469E-18
2.00000E+03	8.90718E-17	4.49334E-18

2.50000E+03	7.31370E-17	3.09439E-18
3.00000E+03	6.20844E-17	2.27211E-18
3.50000E+03	5.39623E-17	1.74543E-18
4.00000E+03	4.77397E-17	1.38674E-18
4.50000E+03	4.28199E-17	1.13099E-18
5.00000E+03	3.88316E-17	9.41753E-19
6.00000E+03	3.27579E-17	6.84911E-19
7.00000E+03	2.83501E-17	5.22475E-19
8.00000E+03	2.50051E-17	4.12856E-19
9.00000E+03	2.23797E-17	3.35197E-19
1.00000E+04	2.02643E-17	2.78059E-19

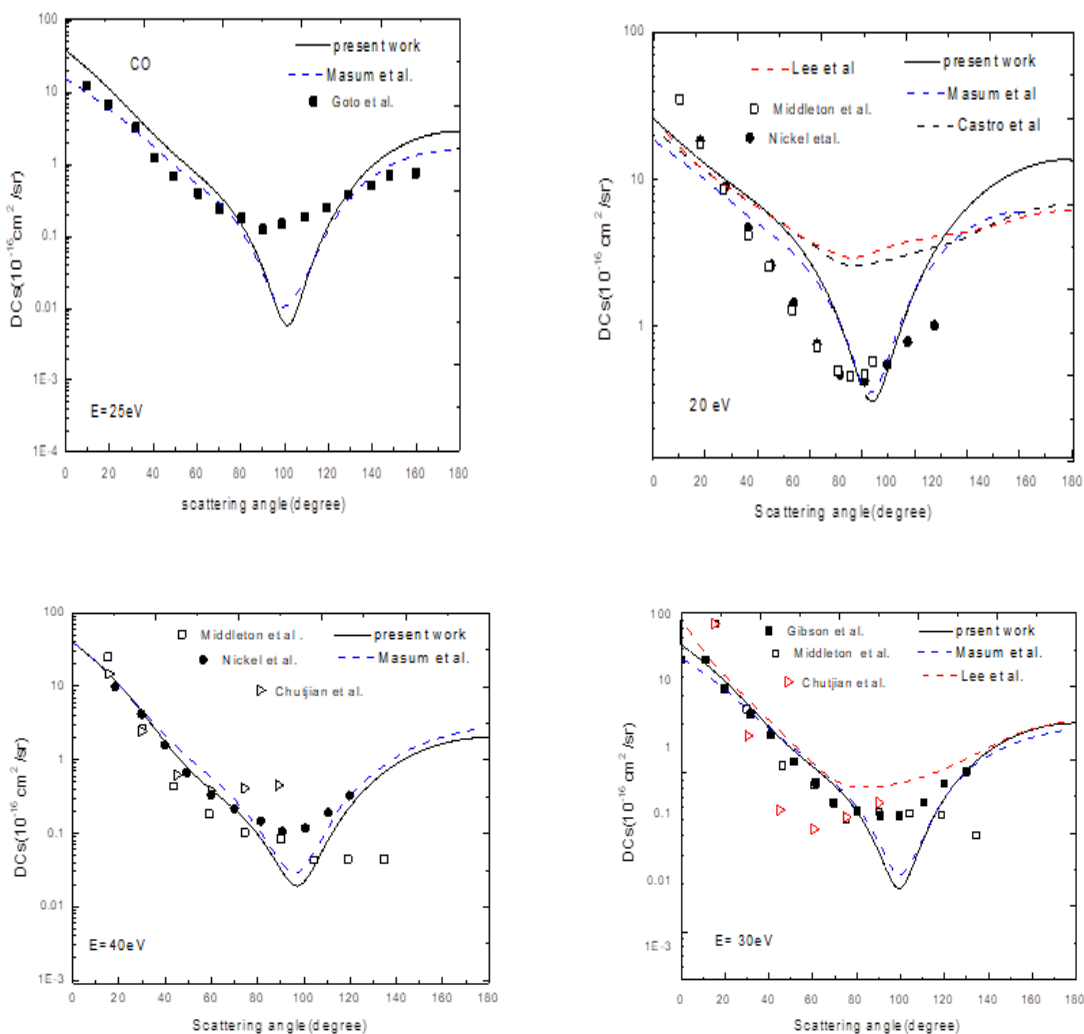


Figure 1: DCS (cm^2 / sr) for elastic scattering of electrons from CO at energies of 20, 25, 30, and 40 eV. Theoretical data for Billah et al. [17], Castro et al.[33], Lee et al. [34]. Experimental data for Middleton et al. [35], Nickel et al. [36], Gibson et al. [37], Chutjian and Tanaka[38].

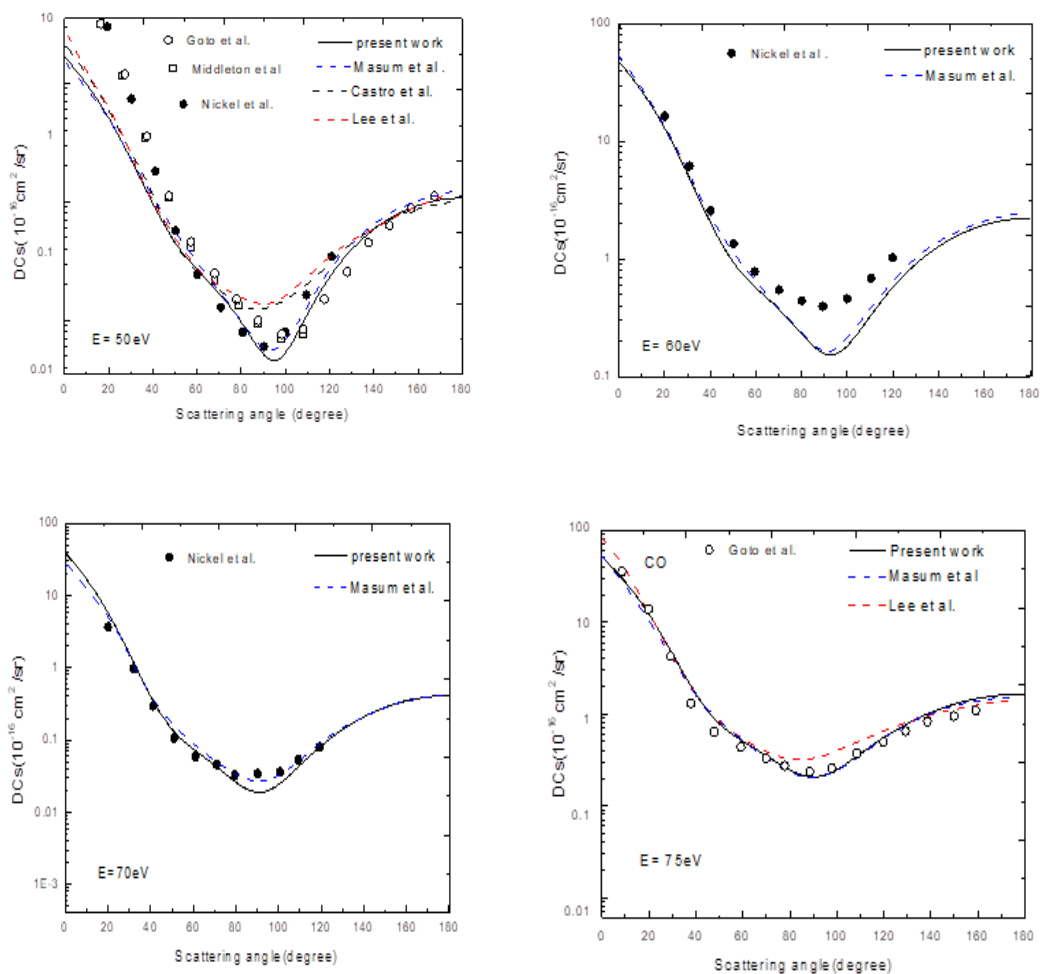


Figure 2: DCS (cm^2/sr) for elastic scattering of electrons from CO at energies 50, 60,70, and 75 eV. Theoretical data for Billah et al. [17], Castro et al. [33], and Lee et al. [34]. Experimental data for Nickel et al. [36], and Gote and Ehrhardt [27]

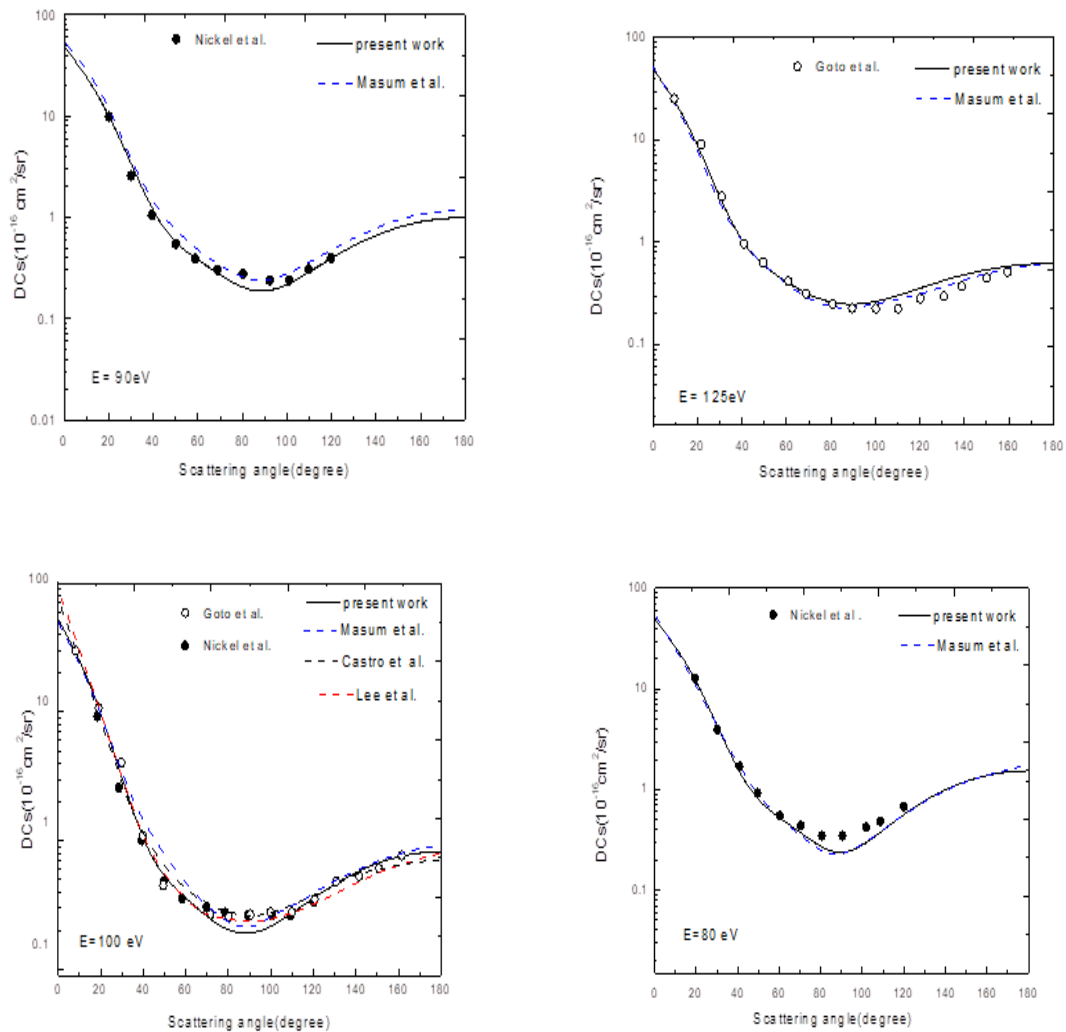


Figure 3: DCS ($10^{-16} \text{ cm}^2 / \text{sr}$) for elastic scattering of electrons from CO at energies 80, 90,100, and 125 eV. Theoretical for Billah et al. [17], Castro et al. [33] and Lee et al. [34]. Experimental for Nickel et al. [36], and Gote and Ehrhardt [27]

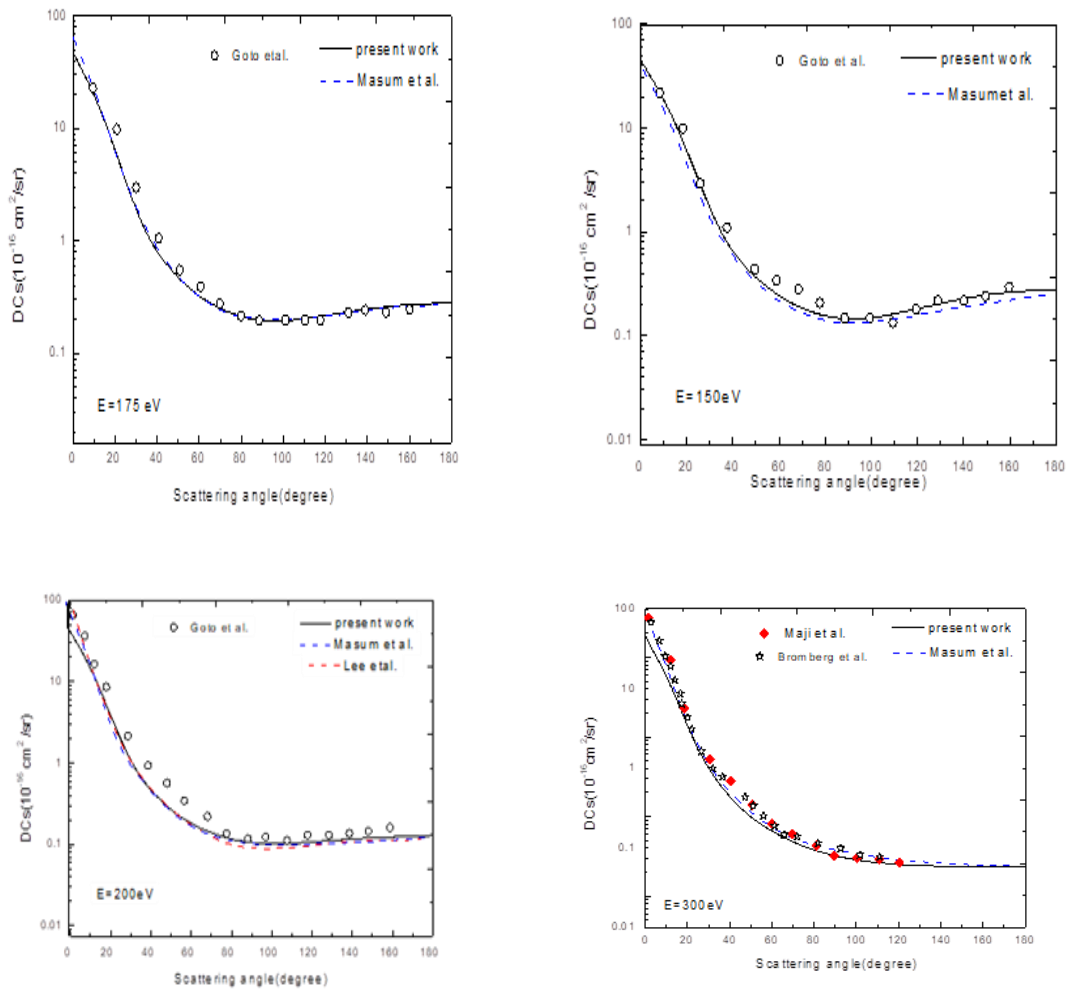


Figure 4: DCS ($10^{-16} \text{ cm}^2/\text{sr}$) for elastic scattering of electrons from CO at energies of 150,175,200 and 300 eV. Theoretical data for Billah et al. [17], Castro et al. [33], and Lee et al. [34]. Experimental for Nickel et al. [36], Gote and Ehrhardt [27], Maji et al. [39], and Bromberg[40]

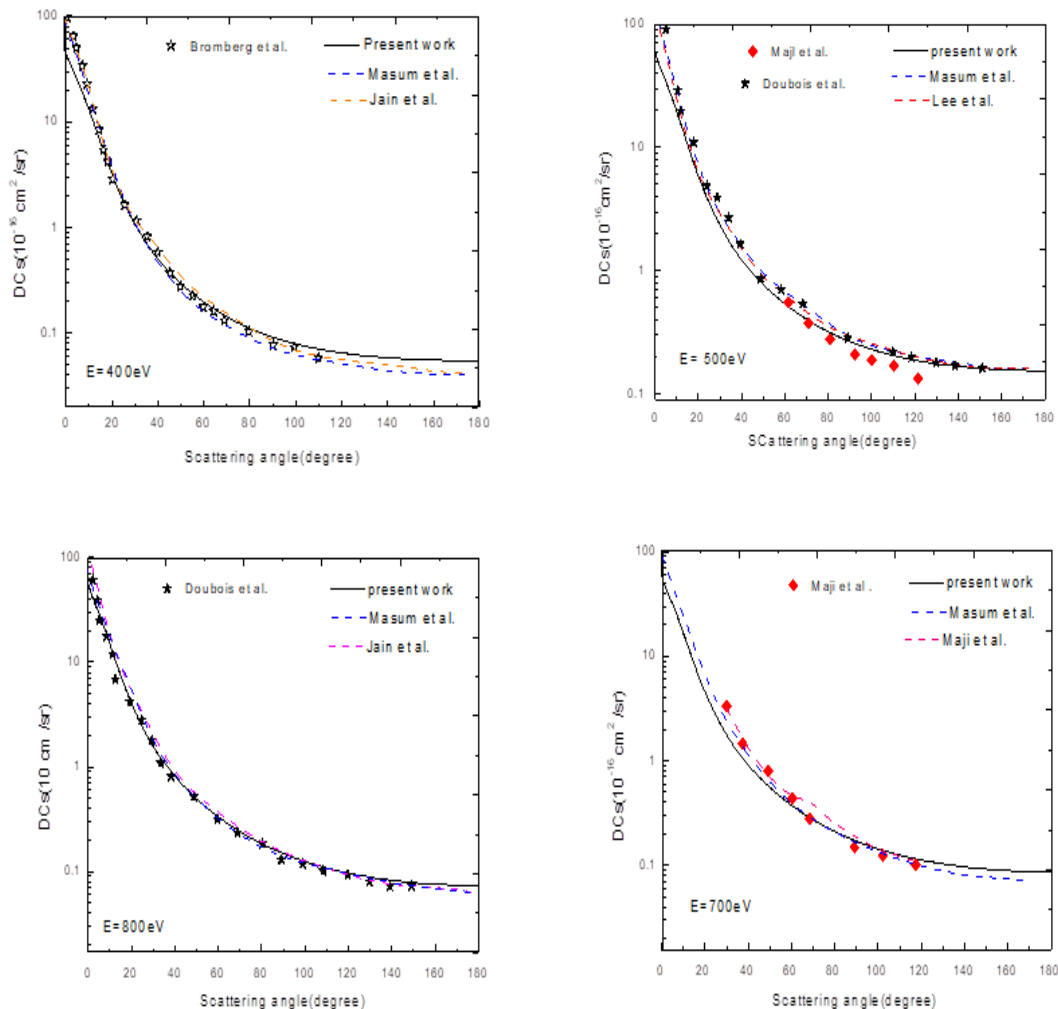


Figure 5: DCS ($10^{-16} \text{ cm}^2/\text{sr}$) for elastic scattering of electrons from CO at energies 400, 500, 700, and 800 eV. Theoretical data for Billah et al. [17], Jain [41], Maji et al. [39] and Lee et al. [34]. Experimental data for Nickel et al. [36], Gote and Ehrhardt [27], Maji et al. [40], DuBois and Rudd [42] and Bromberg [41]

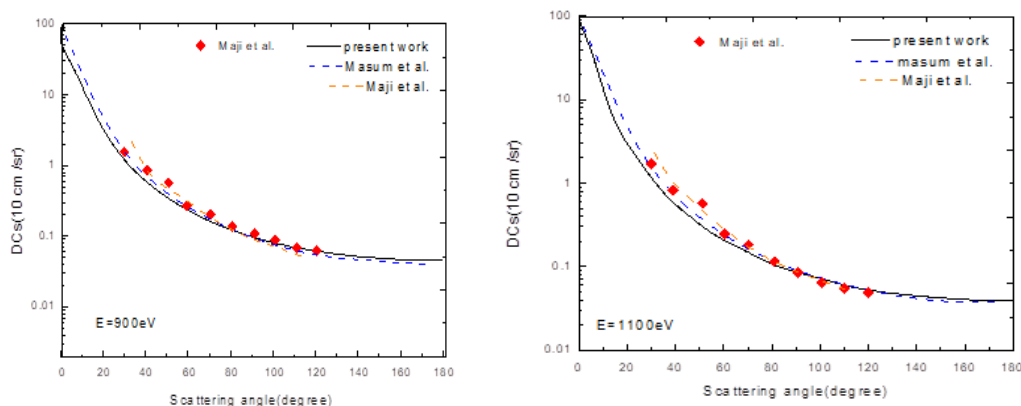


Figure 6: DCS ($10^{-16} \text{ cm}^2/\text{sr}$) for electrons elastic scattering from CO at energies 900 and 1100eV. Theoretical data for Billah et al. [17] and Maji et al. [40]. Experimental from Maji et al. [40]

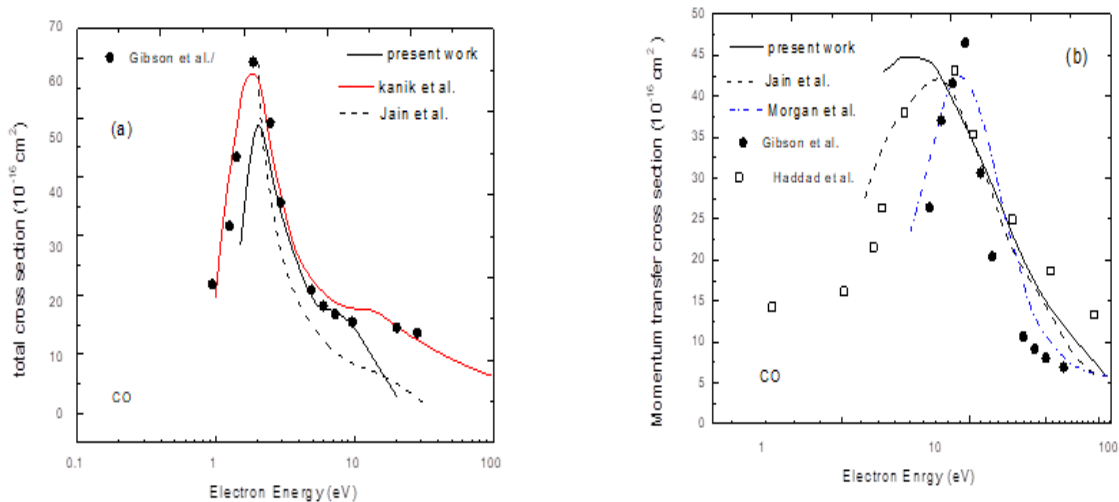


Figure 7: TCS and MTCS for elastic scattering of electrons from CO₂. Theoretical data for Kanik et al. [43], Jain [41] and Morgan and Tennyson[45]. Experimental data from Haddad and Milloy [46] and Gibson et al. [37].

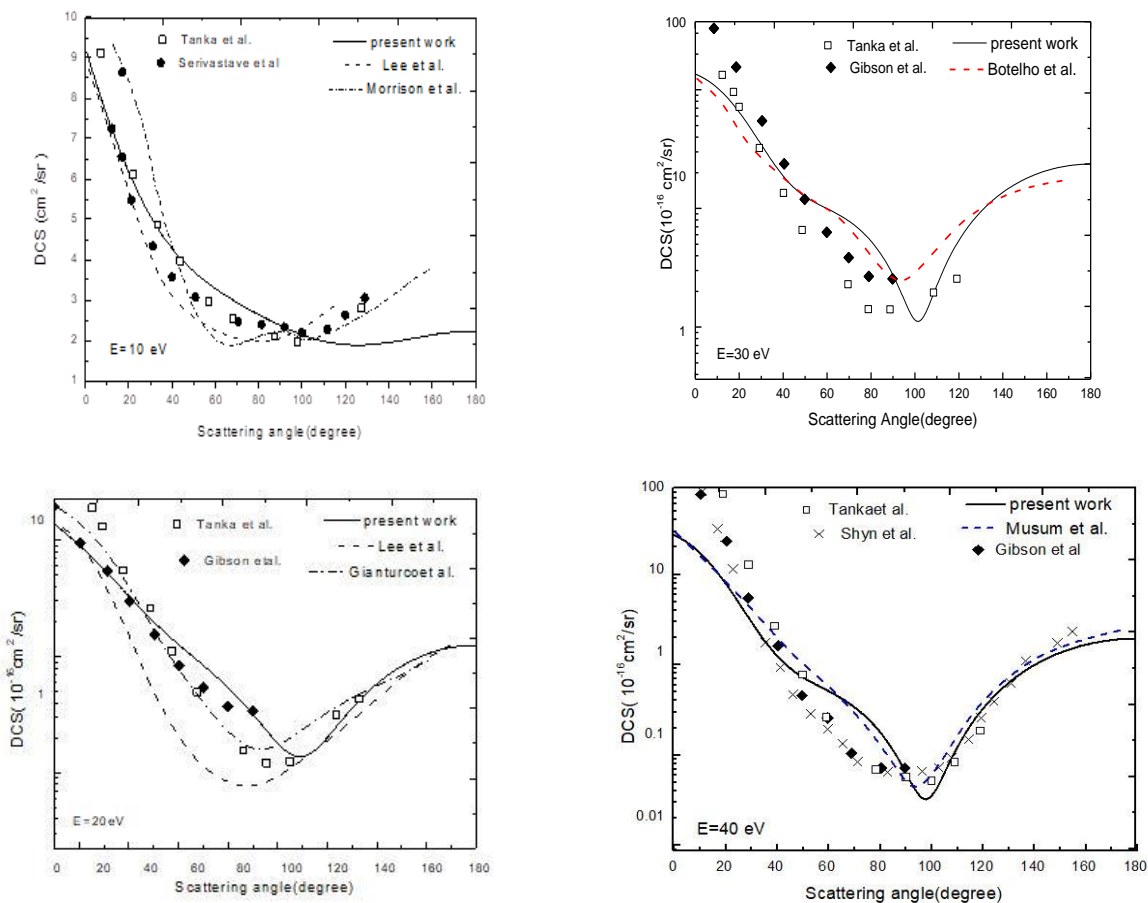


Figure 8: DCS ($10^{-16} \text{cm}^2/\text{sr}$) for elastic scattering of electrons from CO₂ at energies of 10, 20, 30, and 40 eV. Theoretical data for Lee et al. [47], Morrison et al. [48], Gianturco and Paioletti [51], Botelho et al. [4], and Billah et al. [17]. Experimental data for Serivastave et al.[50], Tanaka et al.[49], Gibson et al. [37] and Shyn et al.[52]

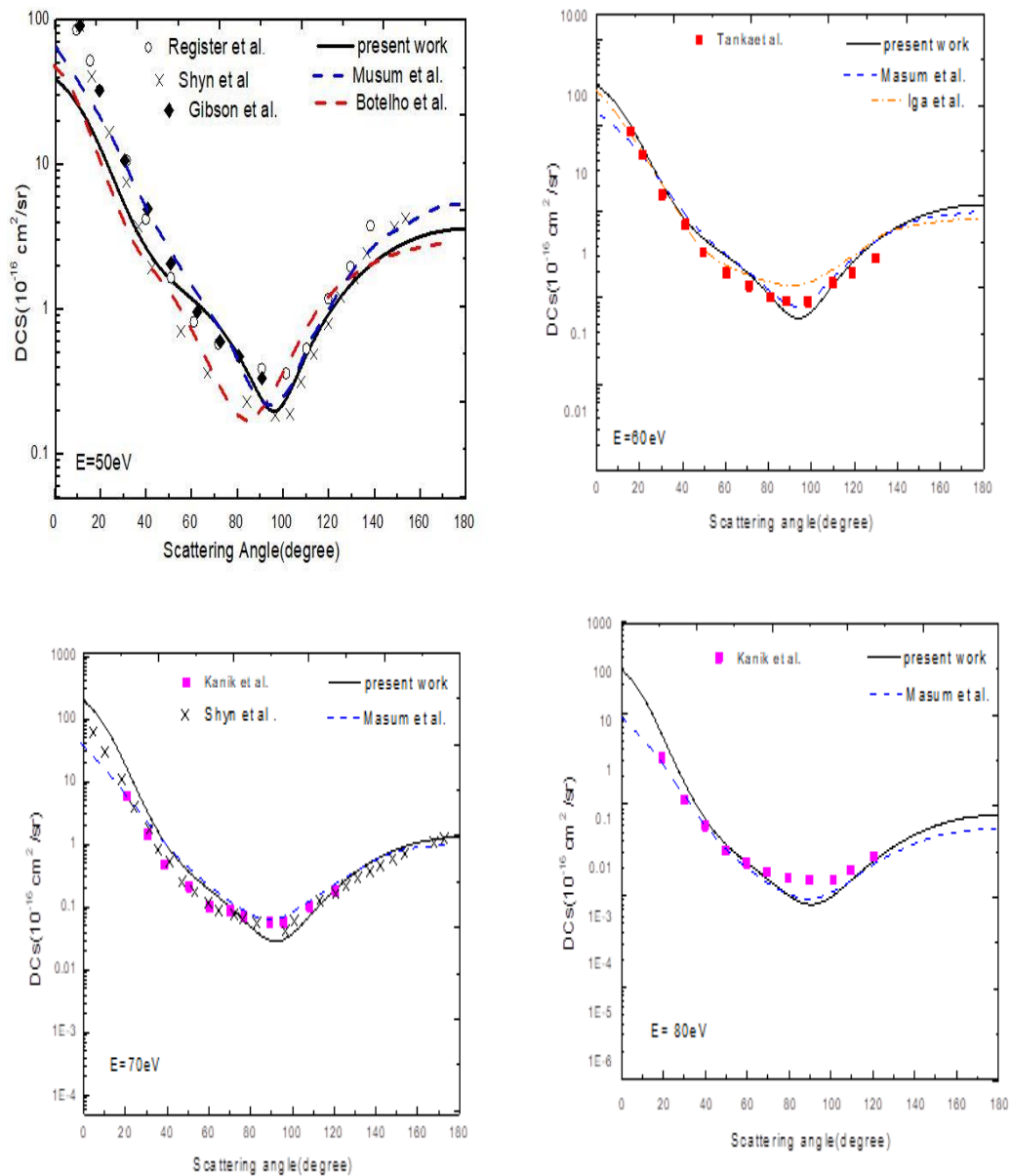


Figure 9: DCS ($10^{-16} \text{ cm}^2/\text{sr}$) for elastic scattering of electrons from CO_2 at energies of 50,60,70 and 80 eV. Theoretical data for Billah et al. [17], Botelho et al. [4], and Iga et al. [56]. Experimental data of Register et al. [53], Shyn et al. [52], Gibson et al. [37], Tanaka et al. [49], and Kanik et al. [55]

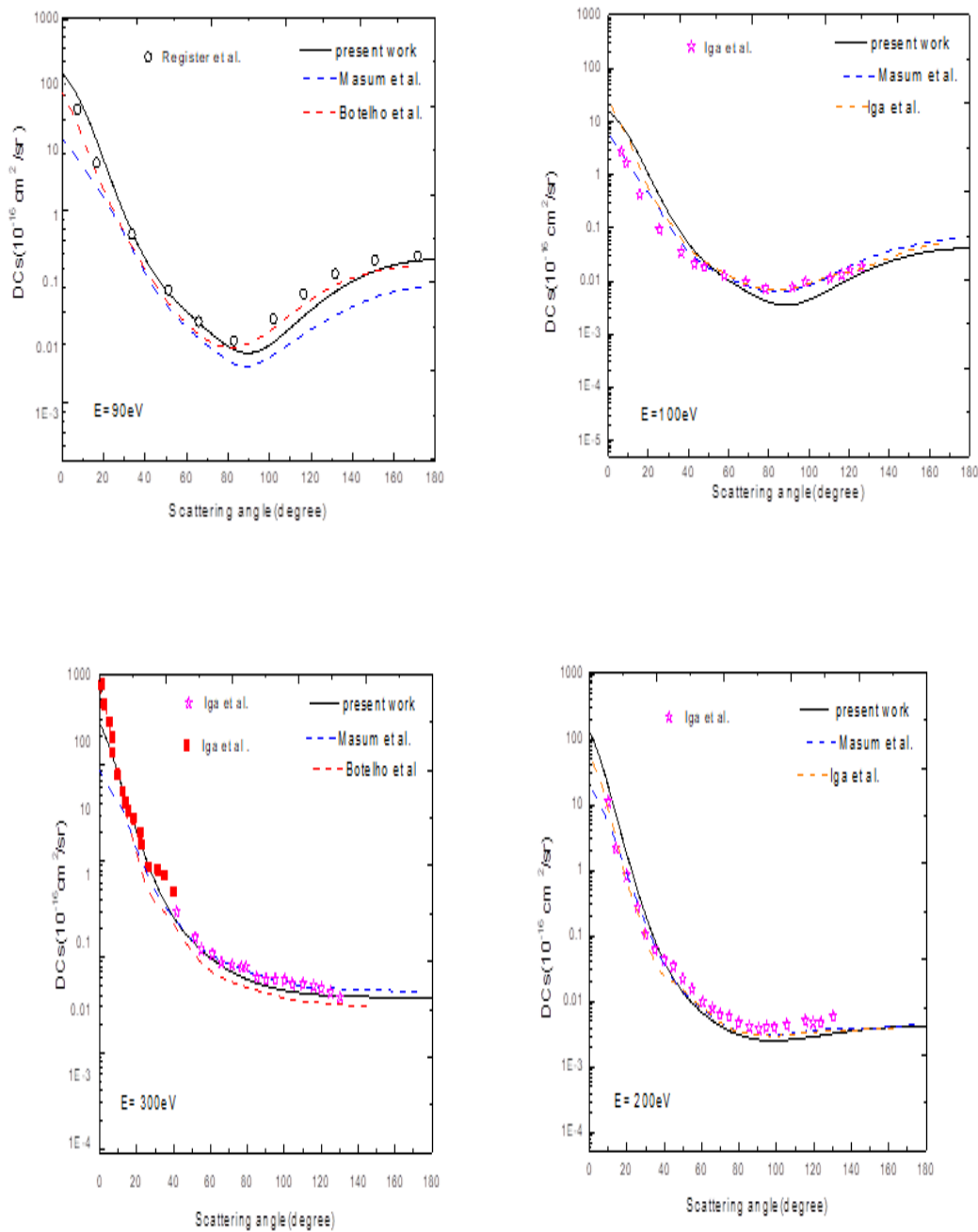


Figure 10: DCS ($10^{-16}\text{cm}^2/\text{sr}$) for elastic scattering of electrons from carbon dioxide at energies of 90,100,200 and 300 eV. Theoretical Masum et al. [17]. Botelho et al. [4], and Iga et al. [54]. Experimental: Register et al. [55] Shyn.[53], Gibson et al. [37] , Iga et al.[54].

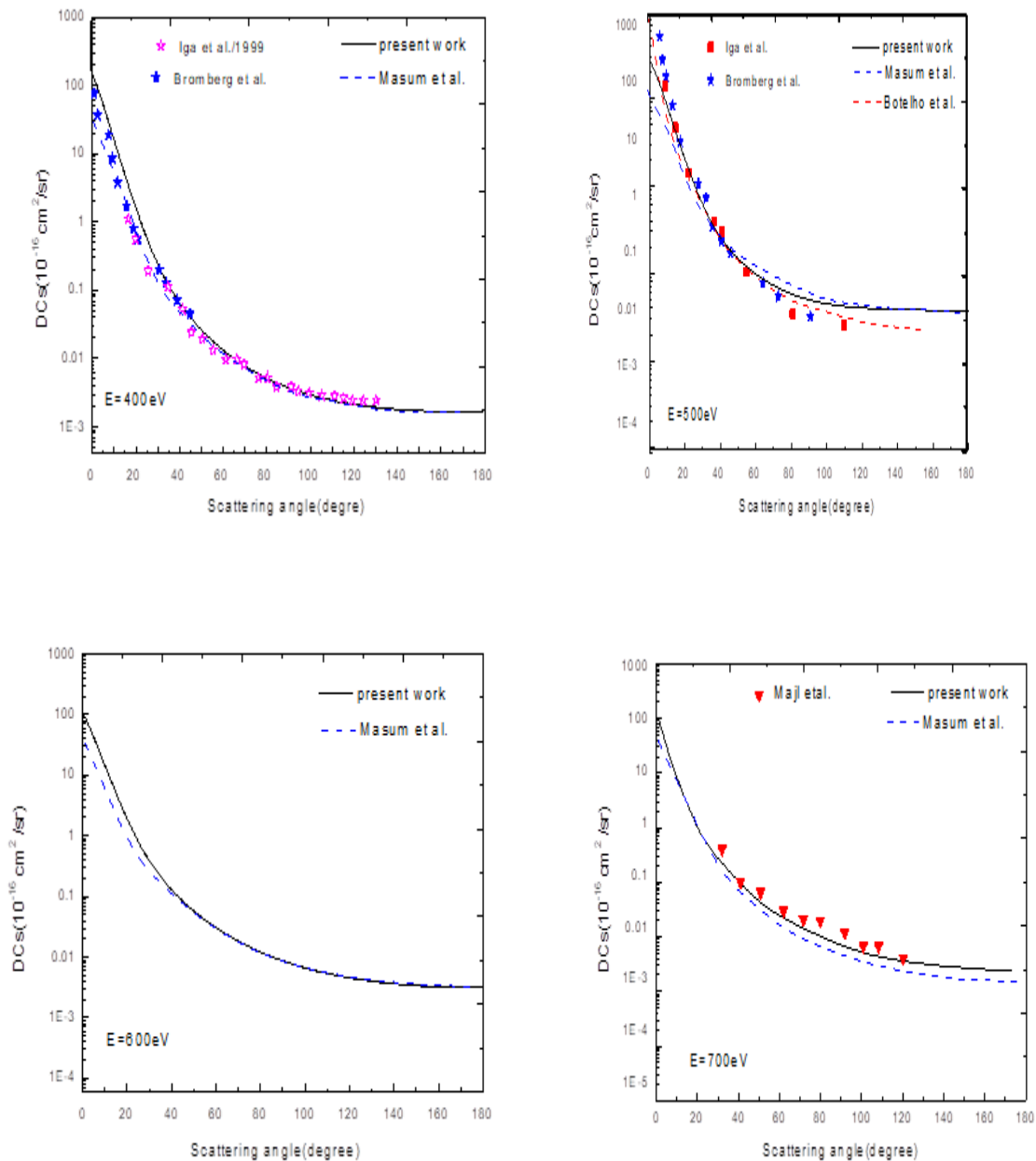


Figure 11: DCS ($10^{-16} \text{ cm}^2/\text{sr}$) for elastic scattering of electrons from CO_2 of 400,500,600 and 700 eV energies. Theoretical data for Billah et al. [17], and Botelho et al. [4]. Experimental data for Iga et al. [54], Bromberg [57] and Maji et al. [39]

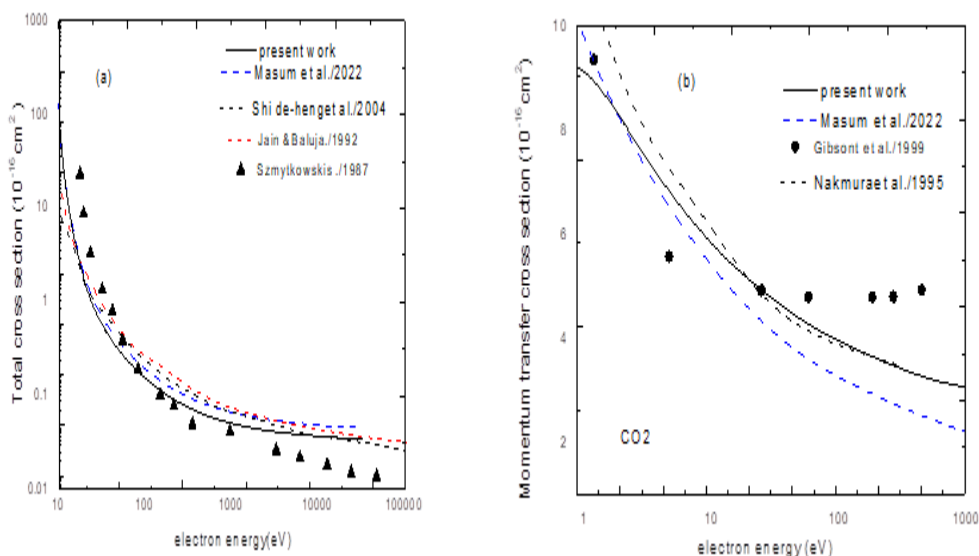


Figure 12: TCS and MTCS for elastic scattering of electrons from CO₂. Theoretical data of Billah et al. [17], De-Heng et al. [58], Nakamura [60] and Jain and Baluja [44]. Experimental data for Szmytkowski and Maciąg [59] and Gibson et al. [37].

Reference

- [1] M. Flannery, "Termolecular Association and Laser-Assisted Electron-(Excited) Atom Collisions," Georgia inst. of tech. Atlanta school of physics, 1991.
- [2] L. G. Christophorou, *Electron—Molecule Interactions and Their Applications: Volume 2*. Academic Press, 2013.
- [3] A. K. Hamoudi, G. N. Flaiyh, and A. N. Abdullah, "Study of Density Distributions, Elastic Electron Scattering form factors and reaction cross sections of 9C, 12N and 23Al exotic nuclei," *Iraqi Journal of Science*, vol. 56, no. 1A, pp. 147-161, 2015.
- [4] L. Botelho, L. Freitas, L. Mu-Tao, A. Jain, and S. Tayal, "Elastic scattering of intermediate and high energy electrons by CO₂," *Journal of Physics B: Atomic and Molecular Physics (1968-1987)*, vol. 17, no. 19, p. L641, 1984.
- [5] A. McWilliam, L. C. Ho, and M. Rauch, *Origin and Evolution of the Elements: Volume 4, Carnegie Observatories Astrophysics Series*. Cambridge University Press, 2004.
- [6] L. Campbell, M. Allan, and M. Brunger, "Electron impact vibrational excitation of carbon monoxide in the upper atmospheres of Mars and Venus," *Journal of Geophysical Research: Space Physics*, vol. 116, no. A9, 2011.
- [7] C. Jackman, R. Garvey, and A. Green, "Electron impact on atmospheric gases, I. Updated cross sections," *Journal of Geophysical Research*, vol. 82, no. 32, pp. 5081-5090, 1977.
- [8] Y. Itikawa and M. Shimizu, "Effective cross sections for collision processes between carbon dioxide and slow electrons, with application to the Martian upper atmosphere," *Bull. Inst. Space and Aeronaut. Sci. Univ. Tokyo*, vol. 7, p. 64, 1971.
- [9] A. A. M. Al-Rahmani and H. A. A. Hussein, "Elastic electron scattering form factors for odd-A 2s-1d shell nuclei," *Iraqi Journal of Science*, vol. 55, no. 4B, 2014.
- [10] Y. Itikawa, "Cross sections for electron collisions with carbon dioxide," *Journal of Physical and Chemical Reference Data*, vol. 31, no. 3, pp. 749-767, 2002.
- [11] H. Tawara, "Atomic and molecular data for H₂O, CO and CO₂ relevant to edge plasma impurities," *Unknown*, 1992.
- [12] T. Shirai, T. Tabata, and H. Tawara, "Analytic cross sections for electron collisions with CO, CO₂, and H₂O relevant to edge plasma impurities," *Atomic Data and Nuclear Data Tables*, vol. 79, no. 1, pp. 143-184, 2001.

- [13] G. P. Karwasz, R. S. Brusa, and A. Zecca, "One century of experiments on electron-atom and molecule scattering: a critical review of integral cross-sections," *La Rivista del Nuovo Cimento*, vol. 24, no. 1, pp. 1-118, 2001.
- [14] M. M. Billah *et al.*, "A Theoretical Study of Scattering of Electrons and Positrons by CO₂ Molecule," *Atoms*, vol. 10, no. 1, p. 31, 2022.
- [15] M. Vinodkumar, C. Limbachiya, and H. Bhutadia, "Electron impact calculations of total ionization cross sections for environmentally sensitive diatomic and triatomic molecules from threshold to 5 keV," *Journal of Physics B: Atomic, Molecular and Optical Physics*, vol. 43, no. 1, p. 015203, 2009.
- [16] J. E. Hudson, C. Vallance, and P. W. Harland, "Absolute electron impact ionization cross-sections for CO, CO₂, OCS and CS₂," *Journal of Physics B: Atomic, Molecular and Optical Physics*, vol. 37, no. 2, p. 445, 2003.
- [17] M. M. Billah *et al.*, "Theoretical investigations of e[±]-CO scattering," *Journal of Physics B: Atomic, Molecular and Optical Physics*, vol. 54, no. 9, p. 095203, 2021.
- [18] M. H. Khandker, A. Haque, M. Maaza, and M. A. Uddin, "Scattering of e[±] from the neon isonuclear series over the energy range 1 eV–0.5 GeV," *Japanese Journal of Applied Physics*, vol. 59, no. SH, p. SHHA05, 2020.
- [19] P. A. M. Dirac, *The principles of quantum mechanics* (no. 27). Oxford university press, 1981.
- [20] F. Salvat, J. Fernández-Varea, and W. Williamson Jr, "Accurate numerical solution of the radial Schrödinger and Dirac wave equations," *Computer physics communications*, vol. 90, no. 1, pp. 151-168, 1995.
- [21] F. Salvat, A. Jablonski, and C. J. Powell, "elsepa—Dirac partial-wave calculation of elastic scattering of electrons and positrons by atoms, positive ions and molecules (New Version Announcement)," *Computer Physics Communications*, vol. 261, p. 107704, 2021.
- [22] A. Jablonski, F. Salvat, and C. J. Powell, "Evaluation of elastic-scattering cross sections for electrons and positrons over a wide energy range," *Surface and Interface Analysis: An International Journal devoted to the development and application of techniques for the analysis of surfaces, interfaces and thin films*, vol. 37, no. 12, pp. 1115-1123, 2005.
- [23] B. Hahn, D. Ravenhall, and R. Hofstadter, "High-energy electron scattering and the charge distributions of selected nuclei," *Physical Review*, vol. 101, no. 3, p. 1131, 1956.
- [24] J. Furness and I. McCarthy, "Semiphenomenological optical model for electron scattering on atoms," *Journal of Physics B: Atomic and Molecular Physics (1968-1987)*, vol. 6, no. 11, p. 2280, 1973.
- [25] J. O'Connell and N. Lane, "Nonadjustable exchange-correlation model for electron scattering from closed-shell atoms and molecules," *Physical Review A*, vol. 27, no. 4, p. 1893, 1983.
- [26] J. P. Desclaux, "A multiconfiguration relativistic Dirac-Fock program," *Computer Physics Communications*, vol. 9, no. 1, pp. 31-45, 1975.
- [27] M. Gote and H. Ehrhardt, "Rotational excitation of diatomic molecules at intermediate energies: absolute differential state-to-state transition cross sections for electron scattering from N₂, Cl₂, CO and HCl," *Journal of Physics B: Atomic, Molecular and Optical Physics*, vol. 28, no. 17, p. 3957, 1995.
- [28] R. Hassan *et al.*, "Scattering of e[±] off silver atom over the energy range 1 eV–1 MeV," *The European Physical Journal D*, vol. 75, no. 7, pp. 1-23, 2021.
- [29] M. Ismail Hossain, A. Haque, M. Atiqur, R. Patoary, M. Uddin, and A. Basak, "Elastic scattering of electrons and positrons by atomic magnesium," *The European Physical Journal D*, vol. 70, no. 2, pp. 1-9, 2016.
- [30] A. Haque *et al.*, "A study of the critical minima and spin polarization in the elastic electron scattering by the lead atom," *Journal of Physics Communications*, vol. 2, no. 12, p. 125013, 2018.
- [31] F. Blanco, L. Ellis-Gibbins, and G. García, "Screening corrections for the interference contributions to the electron and positron scattering cross sections from polyatomic molecules," *Chemical Physics Letters*, vol. 645, pp. 71-75, 2016.
- [32] M. Haque *et al.*, "e[±]Ar scattering in the energy range 1 eV ≤ E_i ≤ 0.5 GeV," *Journal of Physics Communications*, vol. 3, no. 4, p. 045011, 2019.

- [33] E. y Castro, G. de Souza, I. Iga, L. Machado, L. Brescansin, and M.-T. Lee, "Absorption effects for electron-molecule collisions," *Journal of electron spectroscopy and related phenomena*, vol. 159, no. 1-3, pp. 30-38, 2007.
- [34] M.-T. Lee, I. Iga, L. Brescansin, L. Machado, and F. Machado, "Theoretical studies on electron-carbon monoxide collisions in the low and intermediate energy range," *Journal of Molecular Structure: THEOCHEM*, vol. 585, no. 1-3, pp. 181-187, 2002.
- [35] A. Middleton, M. Brunger, and P. Teubner, "Excitation of the electronic states of carbon monoxide by electron impact," *Journal of Physics B: Atomic, Molecular and Optical Physics*, vol. 26, no. 11, p. 1743, 1993.
- [36] J. Nickel, C. Mott, I. Kanik, and D. McCollum, "Absolute elastic differential electron scattering cross sections for carbon monoxide and molecular nitrogen in the intermediate energy region," *Journal of Physics B: Atomic, Molecular and Optical Physics*, vol. 21, no. 10, p. 1867, 1988.
- [37] J. C. Gibson, L. A. Morgan, R. J. Gulley, M. J. Brunger, C. T. Bundschu, and S. J. Buckman, "Low energy electron scattering from CO: absolute cross section measurements and R-matrix calculations," *Journal of Physics B: Atomic, Molecular and Optical Physics*, vol. 29, no. 14, p. 3197, 1996.
- [38] A. Chutjian and H. Tanaka, "Electron impact cross sections for $v=0$ to 1 vibrational excitation in CO at electron energies of 3 to 100 eV," *Journal of Physics B: Atomic and Molecular Physics (1968-1987)*, vol. 13, no. 9, p. 1901, 1980.
- [39] S. Maji, G. Basavaraju, S. Bharathi, K. Bhushan, and S. Khare, "Elastic scattering of electrons by polyatomic molecules in the energy range 300-1300 eV: CO, H and," *Journal of Physics B: Atomic, Molecular and Optical Physics*, vol. 31, no. 22, p. 4975, 1998.
- [40] J. P. Bromberg, "Absolute differential cross sections of elastically scattered electrons. III CO and N₂ at 500, 400, and 300 eV," *The Journal of Chemical Physics*, vol. 52, no. 3, pp. 1243-1247, 1970.
- [41] A. Jain, "Elastic scattering of intermediate-and high-energy electrons by N₂ and CO in the two-potential coherent approach," *Journal of Physics B: Atomic and Molecular Physics (1968-1987)*, vol. 15, no. 10, p. 1533, 1982.
- [42] R. DuBois and M. Rudd, "Differential cross sections for elastic scattering of electrons from argon, neon, nitrogen and carbon monoxide," *Journal of Physics B: Atomic and Molecular Physics (1968-1987)*, vol. 9, no. 15, p. 2657, 1976.
- [43] I. Kanik, S. Trajmar, and J. Nickel, "Total electron scattering and electronic state excitations cross sections for O₂, CO, and CH₄," *Journal of Geophysical Research: Planets*, vol. 98, no. E4, pp. 7447-7460, 1993.
- [44] A. Jain and K. Baluja, "Total (elastic plus inelastic) cross sections for electron scattering from diatomic and polyatomic molecules at 10–5000 eV: H 2, Li 2, HF, CH 4, N 2, CO, C 2 H 2, HCN, O 2, HCl, H 2 S, PH 3, SiH 4, and CO 2," *Physical Review A*, vol. 45, no. 1, p. 202, 1992.
- [45] L. Morgan and J. Tennyson, "Electron impact excitation cross sections for CO," *Journal of Physics B: Atomic, Molecular and Optical Physics*, vol. 26, no. 15, p. 2429, 1993.
- [46] G. Haddad and H. Milloy, "Cross Sections for Electron? Carbon Monoxide Collisions in the Range 1? 4 eV," *Australian journal of physics*, vol. 36, no. 4, pp. 473-484, 1983.
- [47] C.-H. Lee, C. Winstead, and V. McKoy, "Collisions of low-energy electrons with CO 2," *The Journal of chemical physics*, vol. 111, no. 11, pp. 5056-5066, 1999.
- [48] M. A. Morrison, N. F. Lane, and L. A. Collins, "Low-energy electron-molecule scattering: Application of coupled-channel theory to e-C O 2 collisions," *Physical Review A*, vol. 15, no. 6, p. 2186, 1977.
- [49] H. Tanaka *et al.*, "Elastic collisions of low-to intermediate-energy electrons from carbon dioxide: Experimental and theoretical differential cross sections," *Physical Review A*, vol. 57, no. 3, p. 1798, 1998.
- [50] H. Srivastava, P. Jolliffe, and V. Runeckles, "The effects of environmental conditions on the inhibition of leaf gas exchange by NO₂," *Canadian Journal of Botany*, vol. 53, no. 5, pp. 475-482, 1975.
- [51] F. Gianturco and P. Paoletti, "Elastic collisions and rotational excitation in positron scattering from CO 2 molecules," *Physical Review A*, vol. 55, no. 5, p. 3491, 1997.

- [52] T. Shyn, W. Sharp, and G. Carignan, "Angular distribution of electrons elastically scattered from CO₂," *Physical Review A*, vol. 17, no. 6, p. 1855, 1978.
- [53] D. Register, H. Nishimura, and S. Trajmar, "Elastic scattering and vibrational excitation of CO₂ by 4, 10, 20 and 50 eV electrons," *Journal of Physics B: Atomic and Molecular Physics (1968-1987)*, vol. 13, no. 8, p. 1651, 1980.
- [54] I. Iga, J. Nogueira, and L. Mu-Tao, "Elastic scattering of electrons from CO₂ in the intermediate energy range," *Journal of Physics B: Atomic and Molecular Physics (1968-1987)*, vol. 17, no. 6, p. L185, 1984.
- [55] I. Kanik, D. McCollum, and J. Nickel, "Absolute elastic differential scattering cross sections for electron impact on carbon dioxide in the intermediate energy region," *Journal of Physics B: Atomic, Molecular and Optical Physics*, vol. 22, no. 8, p. 1225, 1989.
- [56] I. Iga, M. Homem, K. Mazon, and M. Lee, "Elastic and total cross sections for electron-carbon dioxide collisions in the intermediate energy range," *Journal of Physics B: Atomic, Molecular and Optical Physics*, vol. 32, no. 17, p. 4373, 1999.
- [57] J. P. Bromberg, "Absolute differential cross sections of elastically scattered electrons. V. O₂ and CO₂ at 500, 400, and 300 eV," *The Journal of Chemical Physics*, vol. 60, no. 5, pp. 1717-1721, 1974.
- [58] S. De-Heng, S. Jin-Feng, Y. Xiang-Dong, Z. Zun-Lue, and L. Yu-Fang, "Total cross sections for scattering of electrons from O₂, H₂O, H₂, O₃, CO and CO₂ at 100–2000eV," *Chinese Physics*, vol. 13, no. 7, p. 1018, 2004.
- [59] C. Szmytkowski and K. Maciąg, "Absolute total electron-scattering cross section of SO₂," *Chemical physics letters*, vol. 124, no. 5, pp. 463-466, 1986.
- [60] Y. Nakamura, "Drift Velocity and Longitudinal Diffusion Coefficient of Electrons in CO₂? Ar Mixtures and Electron Collision Cross Sections for CO₂ Molecules," *Australian Journal of Physics*, vol. 48, no. 3, pp. 357-364, 1995.
<https://doi.org/10.1088/0022-3727/20/7/016>